Supplementary Information

Ikaros (*Ikzf1*) mutation confers integrin-dependent survival of pre-B cells and progression to acute lymphoblastic leukemia

by

Ila Joshi, Toshimi Yoshida, Nilamani Jena, Xiaoqing Qi, Jiangwen Zhang,

Richard A. Van Etten, Katia Georgopoulos

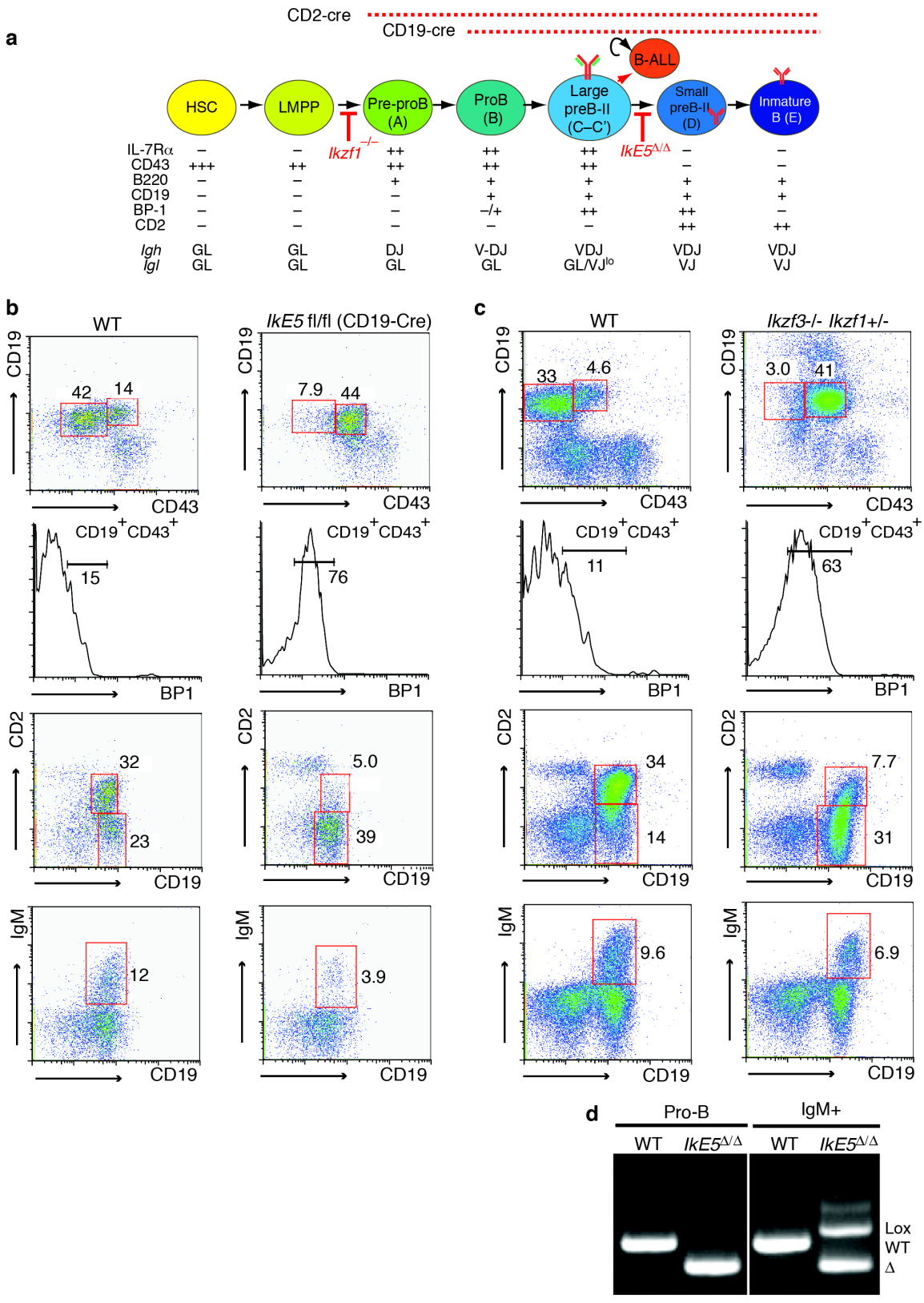

Supplementary Figure 1. Analysis of B-lymphoid differentiation in Ikaros mutant BM.
a, Schematic representation of B cell differentiation as defined by stage-specific markers. Dotted lines indicate differentiation stages with *CD2-* or *CD19-Cre* activity, red lines the differentiation block associated with germline or conditional *Ikaros* gene mutations, and red arrow the stage from which B-ALL is derived. **b-c**, Representative flow cytometric analyses of wild-type (WT), *IkE5*$^{fl/fl}$ *CD19-Cre* (**b**) and *Ikzf3*$^{-/-}$ *Ikzf1*$^{+/-}$ (**c**) BM cells as described in **Fig. 1d**, demonstrating a consistent block at the large pre-B cell stage. *IkE5*$^{fl/fl}$ *CD19-Cre*, *n*=9; *Ikzf3*$^{-/-}$ *Ikzf1*$^{+/-}$, *n*=3. **d**, Deletion analysis of the *Ikzf1* locus in pro-B cells (CD19^{+}CD43^{+}c-Kit^{+}BP1^{-}) and immature B cells (CD19^{+}IgM^{+}) sorted from BM of *IkE5*$^{fl/fl}$ *CD2-Cre* mice.

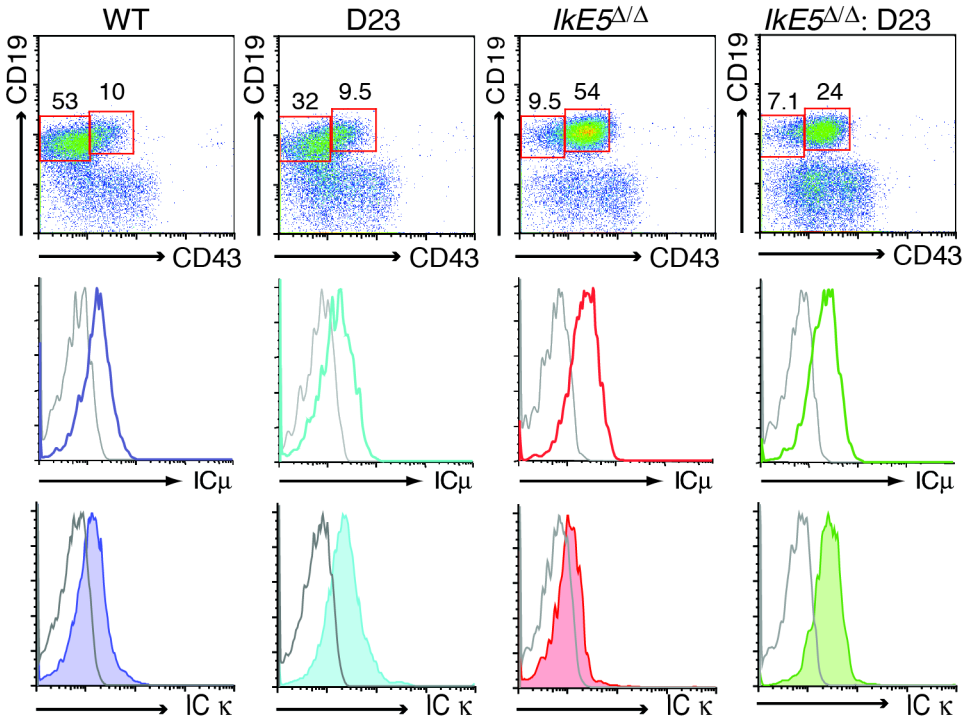

Supplementary Figure 2. Analysis of B-lymphoid differentiation in Igκ-reconstituted Ikaros mutant pre-B cells. Flow cytometric analysis of BM B cells from WT, D23, *IkE5*$^{fl/fl}$ *CD2-Cre* and *IkE5*$^{fl/fl}$ *CD2-Cre*:D23 and intracellular staining for IgM and Igκ in large pre-B cells ($CD19^{+}CD43^{+}BP1^{+}$).

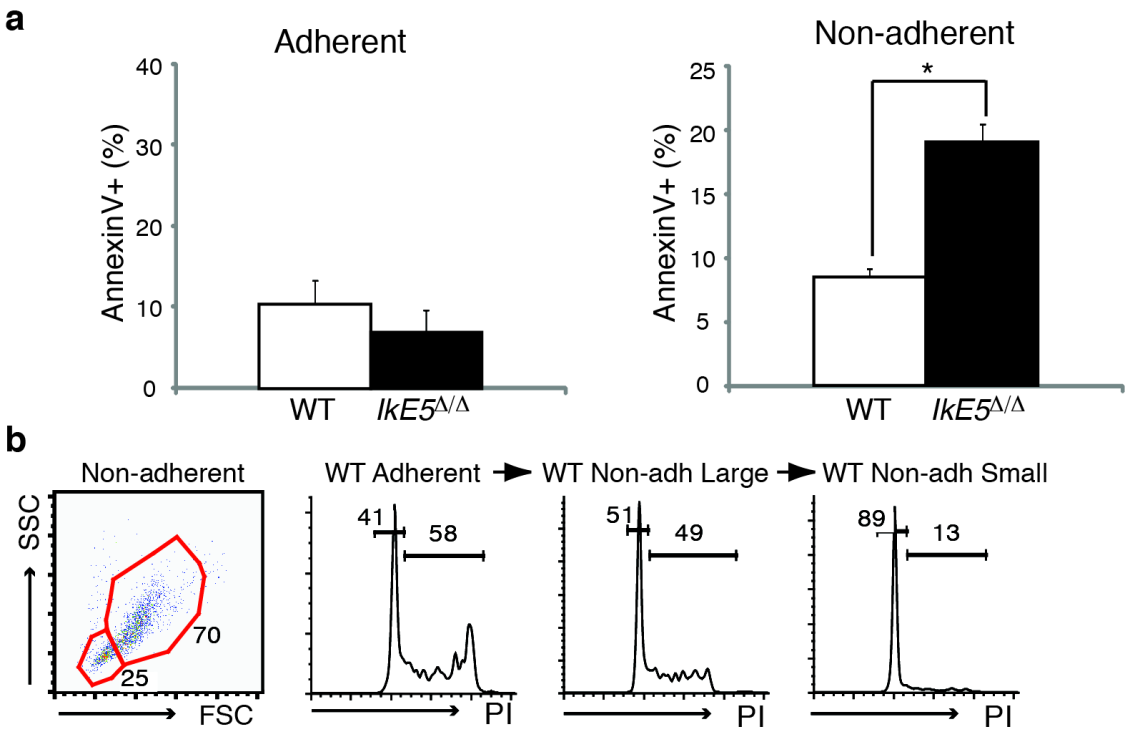

Supplementary Figure 3. Characterization of adherent and non-adherent WT pre-B cells.
a, The mean pro-apoptotic index (percentage of Annexin V^+ cells) of WT and *IkE5*$^{\Delta/\Delta}$ adherent (left panel) and non-adherent (right panel) pre-B cells propagated on OP9 stroma with 5 ng/ml of supplemental IL-7. Asterisk denotes significant changes in apoptosis between WT and mutant pre-B cells (n=2, $^*P < 0.05$). **b**, Representative cell cycle profiles of WT adherent and WT non-adherent pre-B cells grown as in **Fig. 2a**. WT non-adherent pre-B cells were further subdivided according to FSC. The ratio of small vs. large non-adherent WT pre-B in IL-7 cultures increases over time (data not shown). The progressive loss in proliferation in the WT non-adherent pre-B cell phase seen even in the presence of IL-7, suggests a need for stromal contact for maintenance of pre-B cell proliferation. Withdrawal of IL-7 accelerates this process with the ratio of small-non-cycling/large-cycling non-adherent pre-B cells increasing dramatically within 24 hrs (data not shown).

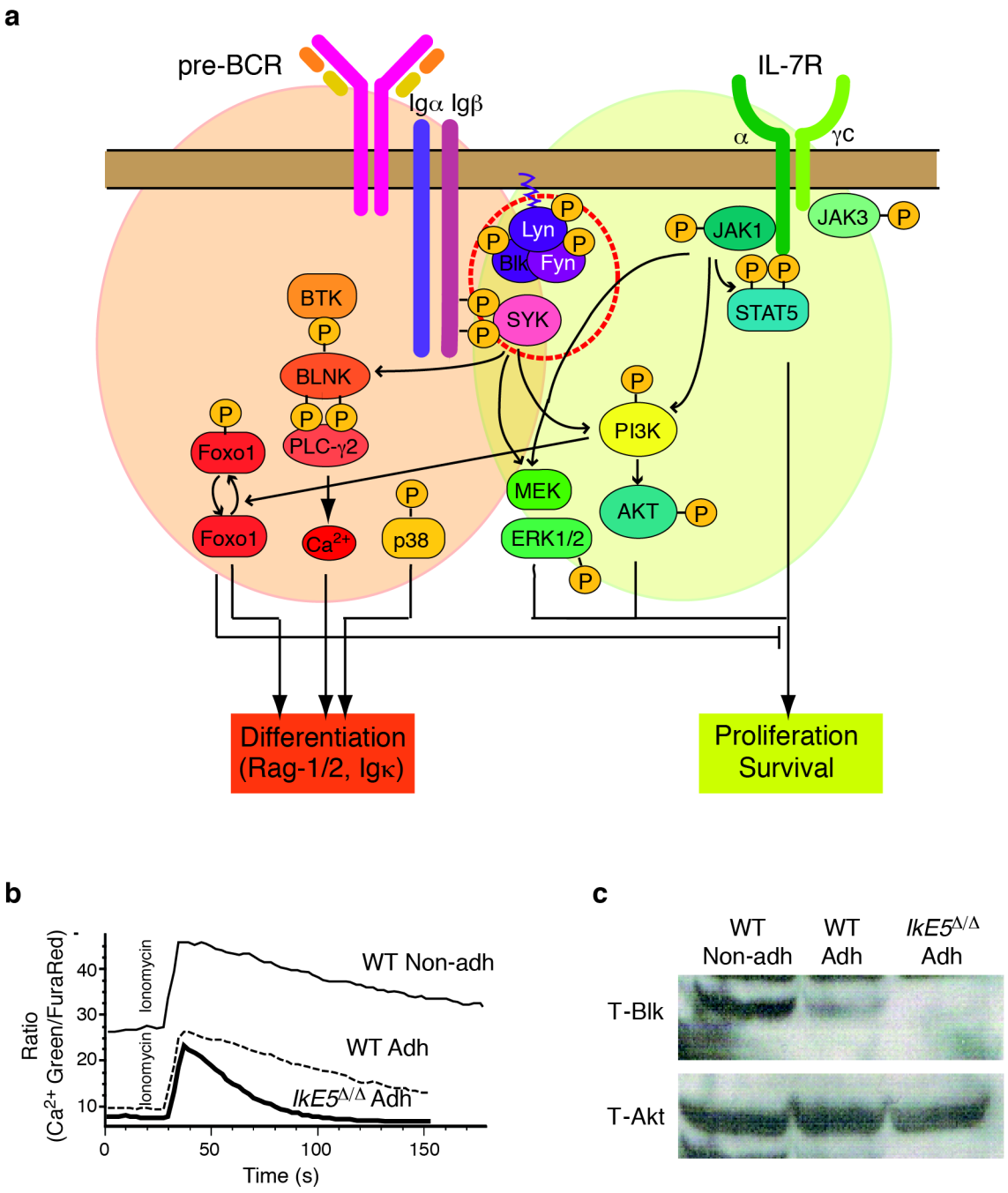

Supplementary Figure 4. Signaling pathways in WT and IKAROS-deficient pre-B cells.
a. Schematic representation of signaling pathways operating downstream of pre-BCR and IL-7R and supporting pre-B cell proliferation, survival and differentiation. Signaling effectors assayed for expression and activity in **Fig. 4a, b** are shown. **b**, Ca^{2+} flux (Ca^{2+} Green/ Fura Red) after ionomycin treatment of WT and *IkE5*$^{\Delta/\Delta}$ adherent and WT non-adherent pre-B cells, n=2. **c**, Total Blk expression is shown for WT and *IkE5*$^{\Delta/\Delta}$ adherent and non-adherent pre-B cells, with total Akt (T-Akt) as loading control.

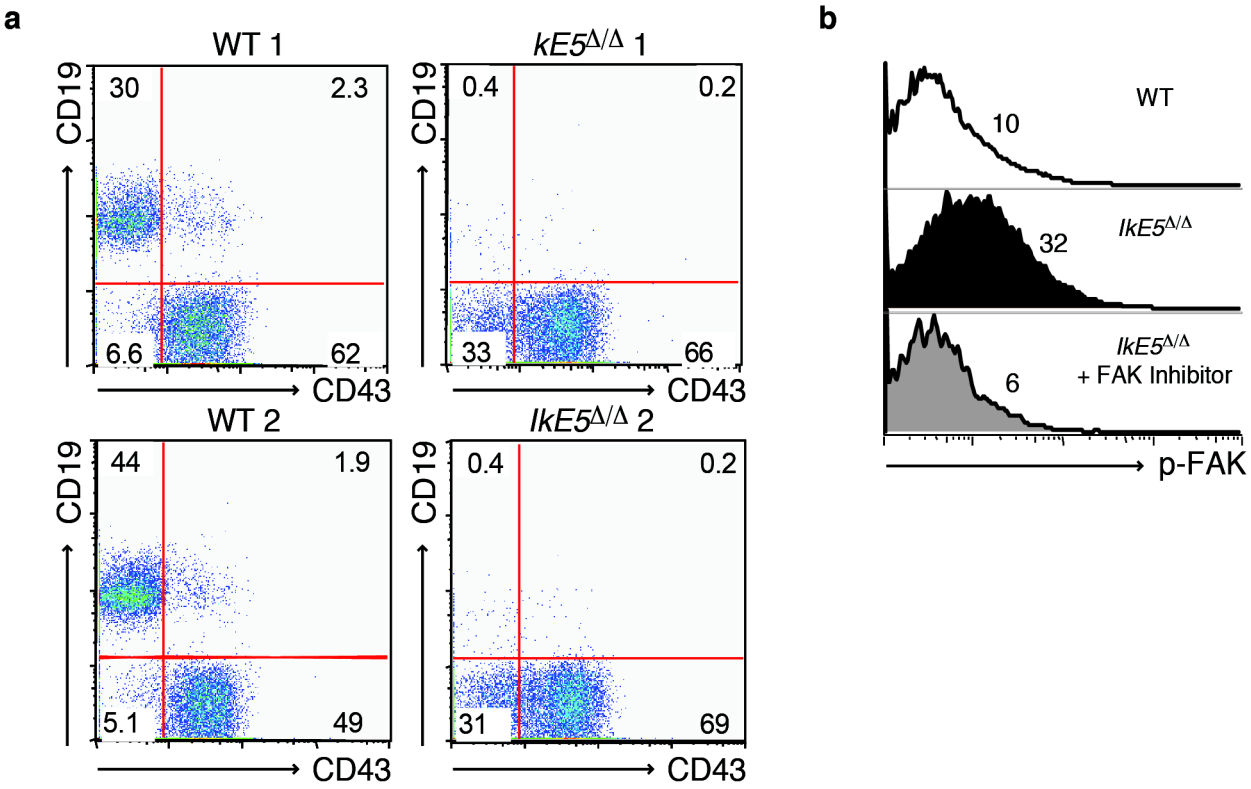

Supplementary Figure 5. Lack of circulating *IkE5*$^{\Delta/\Delta}$ pre-B cells and reduction of p-FAK by FAK inhibitor. **a**, Flow cytometric analysis of peripheral blood from wild-type (WT) and *IkE5*$^{fl/fl}$ *CD19-Cre* mice for large pre-B ($CD19^+CD43^+$) and small pre-B cells ($CD19^+CD43^-$); *n*=2 for each genotype. **b**, FAK inhibitor treatment reduces p-FAK staining in BM *IkE5*$^{\Delta/\Delta}$ pre-B cells, as described in **Fig. 6b**.

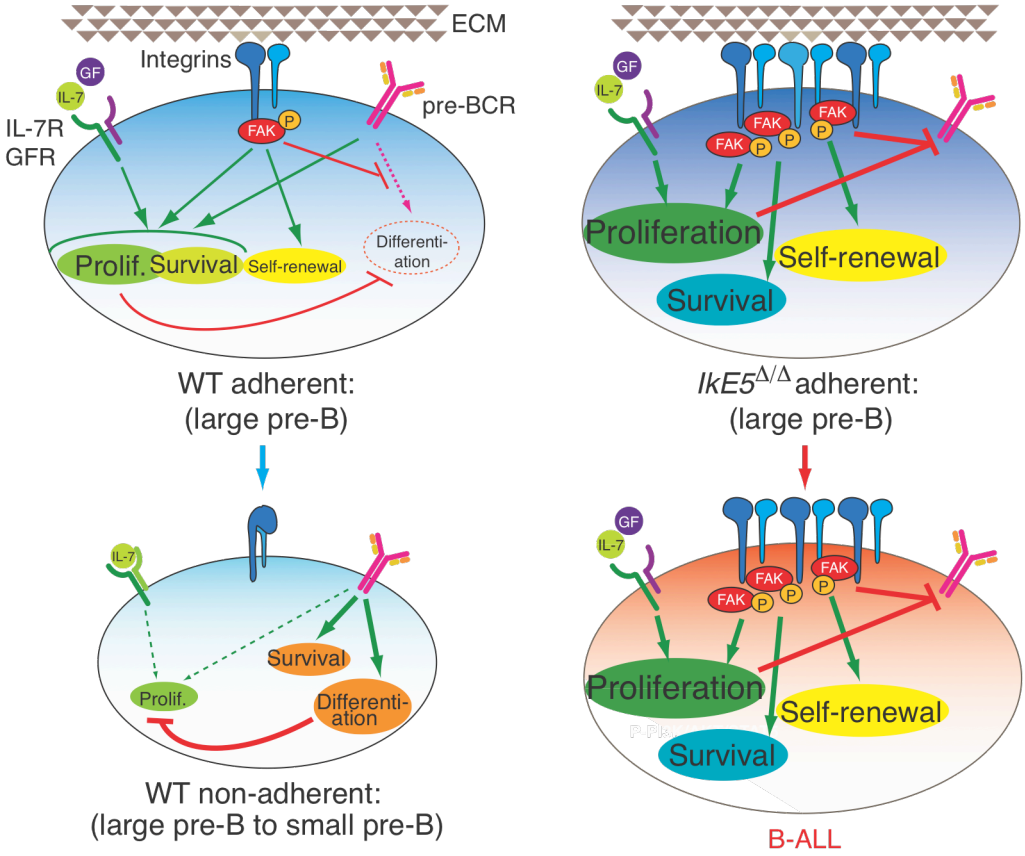

Supplementary Figure 6. Model of pre-BCR, growth factor, and integrin signaling interactions operating during pre-B cell differentiation. Augmentation of integrin signaling by *Ikaros* mutation blocks cells in a stromal-dependent, self-renewing and highly proliferative state where they are unable to differentiate, from which B-ALL arises.

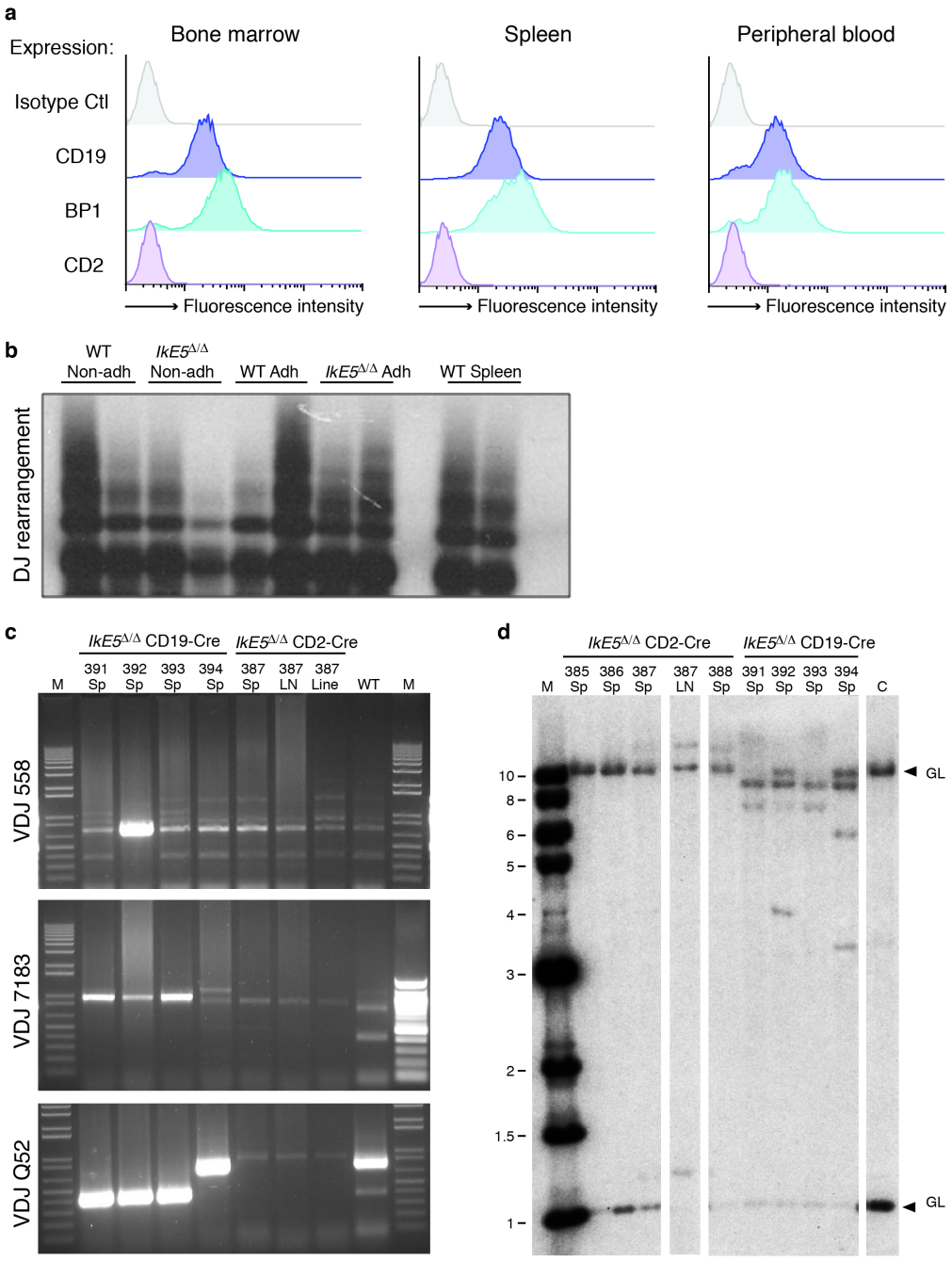

Supplementary Figure 7. Clinicopathological characterization of lymphoid tumors from recipients of *IkE5*$^{\Delta/\Delta}$ pre-B cells. a, Immunophenotypic analysis of precursor B-cell acute lymphoblastic leukemia/lymphoma derived from *IkE5*$^{\Delta/\Delta}$ pre-B cells demonstrates a similar large pre-B cell surface phenotype ($CD19^+CD43^+BP1^+CD2^-$) to the original transplanted population. **b**, Analysis of parental WT and *IkE5*$^{\Delta/\Delta}$ pre-B cell populations (non-adherent and adherent), showing polyclonal *Igh* rearrangements similar to that observed in WT splenocytes. The PCR-based *D-J* rearrangement assay described in **Fig. 1f** was used to determine clonality. PCR products were probed with a *JH*-specific probe. **c**, PCR analysis of *V-D-J* rearrangements in lymphoid tumors from NSG recipients of *IkE5*$^{\Delta/\Delta}$ pre-B cells, as described in **Fig. 1f**. Forward primers from specific *VH* regions (*558*, *Q52*, *7183*) were used in conjunction with a common reverse primer from JH3 (**Fig. 1f**). Note that lymphoid tumors from mice #391, 393, and 394 (from *IkE5*$^{\Delta/\Delta}$ *CD19-Cre* donor) had monoclonal *Igh* rearrangement while #392 tumor had clonal rearrangement of both Igh alleles. **d,** Southern blot analysis of *Igh* gene rearrangements in tissues of leukemic NSG recipients of *IkE5*$^{\Delta/\Delta}$ pre-B cells, as in panel **c**. The position of two germline (GL) *Igh* bands (present in control BM myeloid cells, "C") is denoted by arrowheads. The tissue origin of the sample is indicated (Sp, spleen; LN, lymph node). Common rearrangements between tumors from *IkE5*$^{\Delta/\Delta}$ *CD19-Cre* recipients are indicated by asterisks. Rearrangements in *IkE5*$^{\Delta/\Delta}$ *CD2-Cre* recipients #385 and 386 may not be detected by this probe.